FORMATION AND DEFORMATION OF THE $\psi(3770)$*

S. Coito[a], F. Giacosa[a,b]

[a]Institute of Physics, Jan Kochanowski University
Świętokrzyska 15, 25-406 Kielce, Poland
[b]Institut für Theoretische Physik, Johann Wolfgang Goethe-Universität
Max-von-Laue-Str. 1, 60438 Frankfurt am Main, Germany

(Received September 13, 2017)

The form of resonance line-shapes unveils information about its non-perturbative properties and formation mechanisms. Here, we study the non-Breit–Wigner energy distribution of the resonance $\psi(3770)$ using an unitarized effective Lagrangian approach that includes the effect of the nearby threshold D^+D^-. Two poles are found in the second Riemann sheet near the resonance amplitude. We discuss the setting of the free parameters and possible effects contributing to the signal.

DOI:10.5506/APhysPolBSupp.10.1049

1. Introduction

The resonance $\psi(3770)$ is listed in Particle Data Group with average parameters $M = 3778.1 \pm 1.2$ MeV and $\Gamma = 27.5 \pm 0.9$ MeV [1]. The state is predominantly an $n^{2S+1}L_J = 1^3D_1$ vector charmonium; it is just above the $D\bar{D}$ hadronic decay channel. In Ref. [2], BES data have shown a clearly non-Breit–Wigner line-shape. In other data, such as in BaBar [3] and KEDR [4], such a distortion is also visible, namely a higher slope on the right-hand side of the resonance, while on the left-hand energy side the slope appears to display, in addition, a structure.

One aims to understand the reason for such asymmetries in the line-shape during the formation of the $\psi(3770)$. Interferences due to the $D\bar{D}$ kinematic background are the most obvious to consider, as shown in Ref. [5], justifying the higher slope on the right. The contribution of the $\psi(2S)$ is also taken into account in Refs. [6]. Indeed, it is likely that though dominantly a D-wave, the $\psi(3770)$ is a mixed ${}^3D_1$–${}^3S_1$ state. The inclusion of such an

* Presented by S. Coito at "Excited QCD 2017", Sintra, Lisbon, Portugal, May 7–13, 2017.

effect in itself is not enough to reproduce the structure of the left-hand side of the resonance that has been seen in [2], though, within errors, it is in agreement with the data. In Ref. [7], an estimation of the non-$D\bar{D}$ hadronic background has been performed, though it should be residual. Predictions involving $p\bar{p}$ production, leading to higher cross sections, have been made in Refs. [8, 9]. More within our goal, in Ref. [10] non-perturbative dynamical effects in the formation of the $\psi(3770)$ are studied in an effective Lagrangian model including the $\psi(2S)$, $D\bar{D}$ loops and D–$\bar{D}$ rescattering.

In this study, we analyze the dynamical contribution of the D^+D^- loop to the deformation in the line-shape of the $\psi(3770)$ by employing an unitarized effective Lagrangian model. Moreover, driven by the suggestion in Ref. [2] of a two resonance structure, we study the poles on the second Riemann sheet. Indeed, similar models have been employed to light-meson systems where it has been shown that, besides the regular "seed" pole, extra dynamical poles have been found, alias the $a_0(980)$ [11] and the $\kappa(800)$ [12], leading to deformed line-shapes in the amplitude (for previous work on the subject, see Ref. [13]). Similar phenomena is not forbidden to exist for heavy systems.

2. An effective description of $\psi(3770)$

2.1. The Lagrangian

We consider the decay $\psi(3770) \to D^+D^-$ of a charmonium vector to two pseudoscalars. The interacting Lagrangian density $\mathcal{L}_\mathrm{I}$ is defined by

$$\mathcal{L}_\mathrm{I} = i g_{\psi DD} \psi_\mu \left(\partial^\mu D^+ D^- - \partial^\mu D^- D^+\right) , \tag{1}$$

where the fields ψ, D^+ and D^- are interacting in the space with a coupling $g_{\psi DD}$. (An analogous, here omitted, interaction term couples ψ to $D^0\bar{D}^0$.) This Lagrangian leads to the amplitude $|\mathcal{M}|^2$ for the process $\psi \to D^+D^-$

$$|\mathcal{M}|^2 = \tfrac{4}{3} g_{\psi DD}\ p^2(s) f(p) , \tag{2}$$

where $p(s)$ is the relativistic center-of-mass (CM) momentum of D^+D^-, with s the CM energy squared and $f(p)$ an extra cutoff function that ensures the convergence of the self-energy (defined in Sec. 2.3) with the momentum. We use the damping form

$$f(p) = e^{-2p^2/\Lambda^2} , \tag{3}$$

where Λ is the cutoff parameter. Hence, the model contains two free parameters, $g_{\psi DD}$ and Λ. If we assume Λ to be proportional to the inverse of the size of the wave-function, the Fourier transform of Eq. (3) leads to a Gaussian in coordinate space that models a wave-packet. Therefore, we can estimate the size of our system using a Schrödinger model. Formally, the cutoff function $f(p)$ can be included in the Lagrangian by rendering it non-local [14]; moreover, even if we use a 3D cutoff, the covariance is satisfied, see details in Ref. [15].

2.2. Size of the wave-function

Let us consider the coupled system $c\bar{c}$–D^+D^-, where $c\bar{c}$ is a charmonium system with quantum numbers $^3D_1$, and D^+D^- is a meson–meson decay channel. The wave function is computed following the model in Ref. [16]. For the model parameters "string-breaking" 4.0 GeV^{-1} and coupling 0.8, we find a pole at $3773.1 - i3.4$ MeV to which corresponds a wave-function with r.m.s. value $\sqrt{\langle r^2 \rangle} = 4.74$ GeV^{-1} ~ 0.93 fm. If $\sqrt{\langle r^2 \rangle} \sim 1/\Lambda$, our previously free parameter Λ in (3) is around 211 MeV.

2.3. Spectral functions

The self-energy Σ of a two-meson loop can be written as

$$\Sigma(s) = \Omega(s) + i\sqrt{s}\Gamma(s)\,, \qquad \Omega, \Gamma \in \Re\,, \tag{4}$$

where $\Gamma(s)$ is the width's function of the resonance and it is given (see Ref. [1]) by

$$\Gamma(s) = \frac{1}{8\pi}\frac{p(s)}{s}|\mathcal{M}|^2\,, \tag{5}$$

while the real part Ω can be computed from the width through the Kramers–Krönig dispersion relation

$$\Omega(s) = \frac{1}{\pi}\int_{s_{\rm th}}^{\infty} \frac{\sqrt{s'}\Gamma(s')}{s'-s}\mathrm{d}s'\,. \tag{6}$$

The propagator is given by

$$\Delta(s) = \frac{1}{s - m_\psi^2 + \Sigma(s)}\,, \tag{7}$$

and the spectral function, as a function of the CM energy, by $(E = \sqrt{s}\,)$

$$d_\psi(E) = -\frac{2E}{\pi}\mathrm{Im}\ \Delta(E)\,. \tag{8}$$

To ensure faster convergence of the integral in Eq. (6), we use instead of $\Omega(s)$ the once-subtracted dispersion relation $\Omega_{1S}(s) = \Omega(s) - \Omega(m_\psi^2)$ leading to $\Sigma_1(s) = \Omega_{1S}(s) + i\sqrt{s}\Gamma(s)$. For further details, see Ref. [17].

2.4. Unitarization

In the so-called Källen–Lehmann representation, we have

$$\Delta(s) = \int_0^\infty \mathrm{d}s' \frac{d_S(s')}{s - s' + i\varepsilon} \tag{9}$$

in the limit of $s \to \infty$

$$\frac{1}{s} = \frac{1}{s}\int_0^\infty \mathrm{d}s' d_S(s') \Rightarrow \int_0^\infty \mathrm{d}s' d_S(s') = 1\,, \tag{10}$$

where the left part comes from Eq. (7) considering that $\Sigma(s)$ goes to zero due to the cutoff function.

2.5. Poles

In order to find poles on the second Riemann sheet, we analytically continue the loop function Eq. (4) to the complex plane, and the pole condition is given when the denominator of the propagator (7) is zero, *i.e.*,

$$E^2 - m_{\mathrm{R}}^2 + \Sigma(E) = 0\,, \qquad E \in \mathbb{C}\,, \tag{11}$$

with the energy on the second Riemann sheet.

3. Line-shape and poles

In Fig. 1, we show the unitarized line-shape distribution according to Eq. (8) in D^+D^- channel, using the parameters $m_\psi = 3773.13$ MeV (mass fit in [1]), $\Lambda = 211$ MeV, and $g_{\psi DD} = 44\sqrt{2}$, represented by the solid line. The result reproduces the structure observed in the BES data, namely the higher slope on the higher energy side, and the deformation on the lower energy side. We find two poles corresponding to these parameters: $3744 - i11$ MeV and $3775 - i6$ MeV. Furthermore, we study the influence of the strong coupling $g = g_{\psi DD}$ on the line-shape. For $\tilde{g} = 0.7g$, the line-shape exhibits only one peak, yet with two poles at $3741 - i20$ MeV and $3778 - i3$ MeV. For $\tilde{g} = 1.3g$, the line-shape shows clearly two peaks, corresponding to the poles $3743 - i4$ MeV and $3778 - i9$ MeV. The lower energy pole is generated dynamically and disappears if g is small enough, remaining only the higher energy pole coming from the "seed". For larger g values, the seed pole moves to higher energies while the dynamical pole approaches the threshold. The existence of two poles does not necessarily mean the existence of two different resonances, instead, it means that the

D–$\bar{D}$ pair, more than contributing to the kinematic background only, plays a dynamical role in the formation of the $\psi(3770)$. One of the reasons might be not only because the $\psi(3770)$ is above and close to the $D\bar{D}$ threshold, but also because it is a dominantly D-wave state and, therefore, its wave function is larger than in the case of S-wave states, conferring its properties of lighter systems.

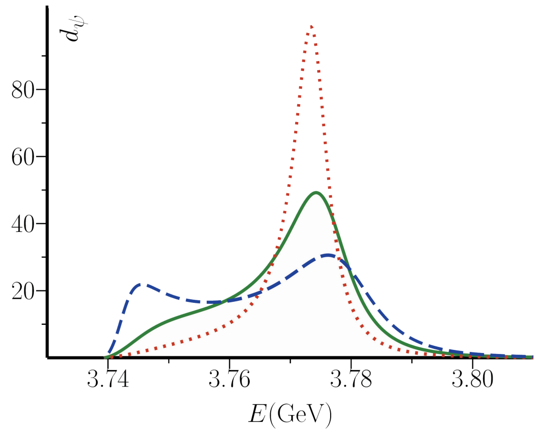

Fig. 1. Line-shape of the resonance $\psi(3770)$ in the D^+D^- channel. Solid line $\tilde{g} = g$, dotted line $\tilde{g} = 0.7g$, and dashed line $\tilde{g} = 1.3g$ (*cf.* the text).

4. Conclusions and outlook

A correct understanding of resonance signals is important to disentangle the non-perturbative phenomena hidden in the line-shapes. Here, we have performed a dynamical study of the $\psi(3770)$ by using an effective Lagrangian model, which points out the relevance of the D^+D^- loop, *viz.* coupled-channel, to the formation of the resonance. We find a two-pole structure in the signal. Further studies include the final-state rescattering, the influence of the cutoff function, and the lepton–lepton decay widths.

We thank the organizers for the very nice workshop and M. Piotrowska, T. Wolkanowski-Gans, G. Rupp, and E. van Beveren for useful discussions. This work was supported by the National Science Centre, Poland (NCN) through the OPUS project No. 2015/17/B/ST2/01625.

REFERENCES

[1] C. Patrignani *et al.* [Particle Data Group], *Chin. Phys. C* **40**, 100001 (2016).

[2] M. Ablikim *et al.* [BES Collaboration], *Phys. Rev. Lett.* **101**, 102004 (2008).

[3] B. Aubert *et al.* [BaBar Collaboration], *Phys. Rev. D* **76**, 111105(R) (2007).

[4] V.V. Anashin *et al.*, *Phys. Lett. B* **711**, 292 (2012).

[5] E. van Beveren, G. Rupp, *Phys. Rev. D* **80**, 074001 (2009).

[6] N.N. Achasov, G.N. Shestakov, *Phys. Rev. D* **86**, 114013 (2012); **87**, 057502 (2013).

[7] G. Li, X.H. Liu, Q. Wang, Q. Zhao, *Phys. Rev. D* **88**, 0140110 (2013).

[8] J. Haidenbauer, G. Krein, *Phys. Rev. D* **91**, 114022 (2015).

[9] H. Xu, J.J. Xie, X. Liu, *Eur. Phys. J. C* **76**, 192 (2016); A.I. Ahmadov, Yu.M. Bystritskiy, E.A. Kuraev, P. Wang, *Nucl. Phys. B* **888**, 271 (2014).

[10] G.Y. Chen, Q. Zhao, *Phys. Lett. B* **718**, 1369 (2013).

[11] T. Wolkanowski, F. Giacosa, D.H. Rischke, *Phys. Rev. D* **93**, 014002 (2016).

[12] T. Wolkanowski, M. Sołtysiak, F. Giacosa, *Nucl. Phys. B* **909**, 418 (2016).

[13] N.A. Tornqvist, *Z. Phys. C* **68**, 647 (1995); M. Boglione, M.R. Pennington, *Phys. Rev. D* **65**, 114010 (2002); E. van Beveren *et al.*, *Z. Phys. C* **30**, 615 (1986).

[14] J. Terning, *Phys. Rev. D* **44**, 887 (1991); G.V. Efimov, M.A. Ivanov, *The Quark Confinement Model of Hadrons*, Bristol, UK: IOP, p. 177, 1993; Y.V. Burdanov, G.V. Efimov, S.N. Nedelko, S.A. Solunin, *Phys. Rev. D* **54**, 4483 (1996); A. Faessler *et al.*, *Phys. Rev. D* **68**, 014011 (2003); F. Giacosa, T. Gutsche, A. Faessler, *Phys. Rev. C* **71**, 025202 (2005).

[15] M. Sołtysiak, F. Giacosa, *Acta Phys. Pol. B Proc. Suppl.* **9**, 467 (2016).

[16] S. Coito, *Phys. Rev. D* **94**, 014016 (2016).

[17] F. Giacosa, G. Pagliara, *Phys. Rev. C* **76**, 065204 (2007).